Characterization of Carbon Nanotube Fiber Compressive Properties Using Tensile Recoil Measurement

Mei Zu,[†,‡] Weibang Lu,[‡,*] Qing-Wen Li,[§] Yuntian Zhu,[⊥] Guojian Wang,[†] and Tsu-Wei Chou[‡,*]

[†]School of Materials Science and Engineering, Tongji University, Shanghai 201804, China, [‡]Department of Mechanical Engineering and Center for Composite Materials, University of Delaware, Newark, Delaware 19716, United States, [§]Suzhou Institute of Nano-Tech and Nano-Bionics, Suzhou 215123, China, and [⊥]Department of Materials Science and Engineering, North Carolina State University, Raleigh, North Carolina 27695, United States

ABSTRACT

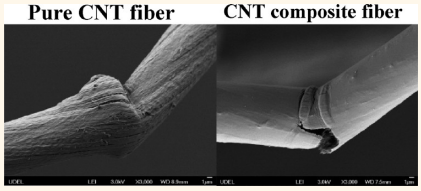

The tensile properties of carbon nanotube (CNT) fibers have been widely studied. However, the knowledge of their compressive properties is still lacking. In this work, the compressive properties of both pure CNT fibers and epoxy infiltrated CNT fibers were studied using the tensile recoil measurement. The compressive strengths were obtained as 416 and 573 MPa for pure CNT fibers and CNT–epoxy composite fibers, respectively. In addition, microscopic analysis of the fiber surface morphologies revealed that the principal recoil compressive failure mode of pure CNT fiber was kinking, while the CNT–epoxy composite fibers exhibited a failure mode in bending with combined tensile and compressive failure morphologies. The effect of resin infiltration on CNT fiber compressive properties, including the compressive strength and the deformation mode, is discussed. This work expands the knowledge base of the overall mechanical properties of CNT fibers, which are essential for their application in multifunctional composites.

KEYWORDS: carbon nanotube fibers · composite fibers · tensile recoil measurement · compressive behavior · resin infiltration

Carbon nanotube (CNT) fibers have attracted considerable research interests due to their simple fabrication processes, novel internal structures, as well as remarkable properties.[1−3] They can be fabricated by spinning continuously from CNT solutions,[4−6] CNT aerogels,[7−9] and CNT arrays.[10−12] CNT fibers can be several kilometers long, and their diameters can be as small as several micrometers. The specific elastic moduli and tensile strengths of CNT fibers are now surpassing those of traditional carbon fibers,[9,13,14] mainly due to the highly aligned and densely packed CNTs within them. Thus, one of the most promising applications of CNT fibers is in their use as reinforcements in multifunctional composites. In the past few years, the tensile properties of CNT fibers have been widely studied, mostly by performing single-fiber tensile tests.[1,2] Recently, the interfacial behavior of the CNT fiber/epoxy composite has also been investigated through single-fiber fragmentation test[15] and microdroplet test,[16] which demonstrates a much different interfacial failure mechanism from that of carbon and glass fiber/epoxy composites.

The limited compressive strength of commercial carbon or polymeric fibers often hampers their application in composites under severe loading conditions. The compressive properties of traditional fibers can be characterized by several techniques,[17] such as the elastic-loop test,[18] bending-beam test,[19] tensile recoil test,[20] and single-fiber composite test.[21] Although the tensile properties of CNT fibers have been well studied, there is a lack of understanding of their behavior under axial compression, due to the difficulty in performing compressive tests on such microscale fibers. By performing the single-fiber composite test, Gao *et al.* have reported the reinforcing efficiency of a CNT fiber embedded in the polymer matrix under thermal-induced compression.[22] They concluded that the apparent compressive modulus of the embedded CNT fiber was much higher than that of embedded high modulus carbon fiber, and CNT fiber could continuously carry the compressive loading at large strain without permanent deformation and fracture. This behavior was attributed to the remarkable intrinsic flexibility of CNTs and the coupling effect between CNTs and their surrounding polymer.

Single-fiber composite tests often require tedious procedures for specimen fabrication,

* Address correspondence to chou@udel.edu, weibang@udel.edu.

Received for review February 26, 2012 and accepted April 11, 2012.

Published online April 11, 2012
10.1021/nn300857d

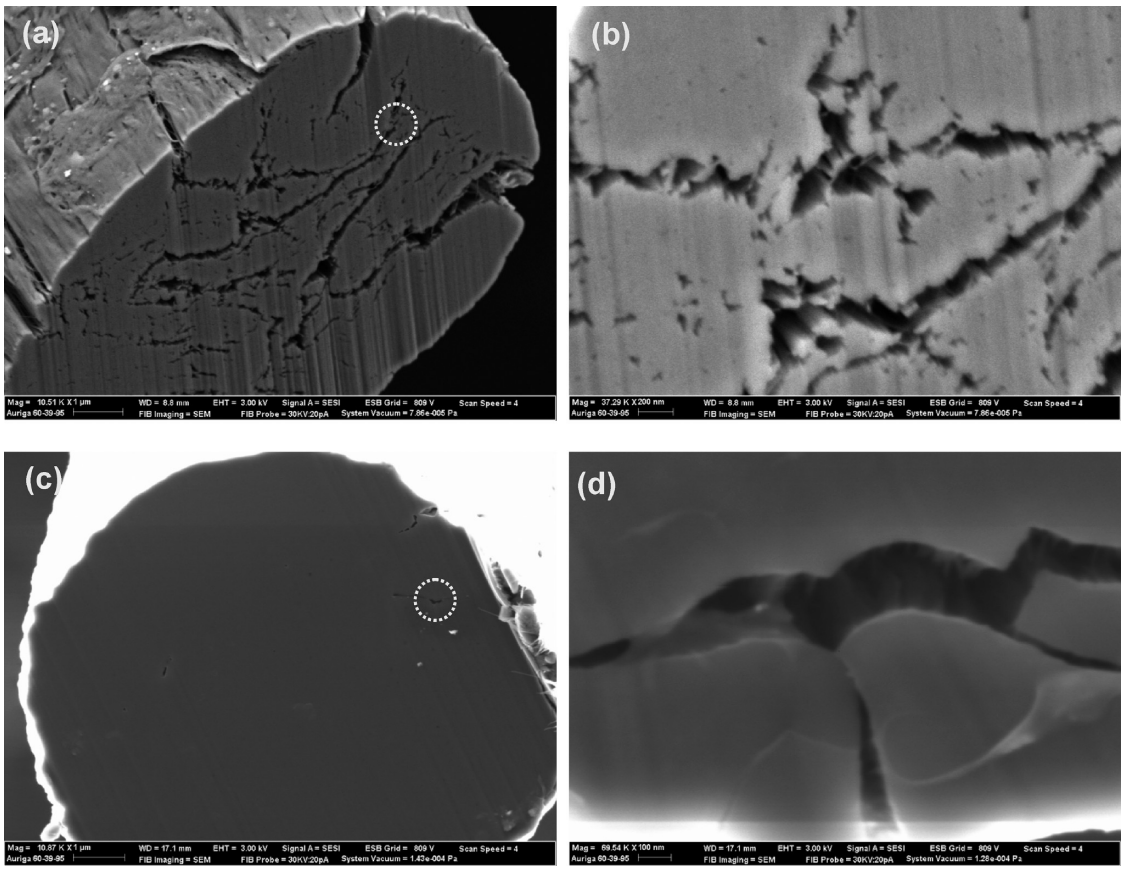

Figure 1. Morphology of the cross sections of a CNT fiber before and after epoxy resin infiltration. (a) Cross section of pure CNT fiber with several crack-like features, (b) an enlargement of the crack-like features in (a), (c) cross section of CNT–epoxy composite fiber with a small number of crack-like features, and (d) an enlargement of the crack-like feature in (c).

and it is difficult to obtain the true compressive strength of an individual fiber from this kind of test. Tensile recoil test, however, is a more direct method of studying the compressive strength of single fibers. The basic principle of tensile recoil test is that, upon tensile fracture, the recoil forces acting upon the two broken fiber segments cause significant fiber damage. According to the procedures developed by Allen,[20] the fiber specimens are cut at various tensile loading levels to identify the threshold at which a cut fiber segment fails, either in buckling, kinking, or fracture, under the recoil compressive loading. By using this method, the compressive strengths and failure mechanisms of several kinds of polymeric fibers and carbon fibers have been obtained.[20,23,24] Recently, our group reported that, after tensile failure, the two segments of the aerogel-spun CNT fibers were either intact or kinked due to the recoil compressive force. Therefore, according to Allen's theory, the compressive strength of those fibers were considered to be equal to their tensile strength, which was around 175 MPa.[25]

In order to gain a better understanding of the overall mechanical properties of CNT fibers, we report a study of the compressive behavior of fibers spun from CNT arrays using the single-fiber tensile recoil test. The compressive strength of CNT fibers is obtained, and their failure mechanisms have been identified using scanning electron microscopy (SEM). Furthermore, our recent study of CNT fiber/polymer interfacial properties concluded that the polymer matrix can infiltrate into the CNT fibers, resulting in enhanced load transfer efficiency between CNTs within the fibers. Hence, in this work, the compressive properties of epoxy infiltrated CNT fibers, termed as CNT–epoxy composite fibers, are also studied using the tensile recoil test. The effect of polymer infiltration on the fiber compressive properties is discussed.

RESULTS AND DISCUSSION

Evaluation of Resin Infiltration in CNT–Epoxy Composite Fibers. CNT fibers tested in this study were spun by drawing and twisting of CNT strips out of vertically well-aligned CNT arrays (forests),[26] whose CNTs were mainly double- and triple-walled with diameters of ~6 nm. CNT–epoxy composite fibers were prepared using a soaking technique.[27] A focused ion beam (FIB) combined with an SEM (Auriga 60 CrossBeam FIB-SEM, Carl Zeiss Microscopy) was used to examine and compare the cross-sectional morphologies of CNT fibers before and after epoxy resin infiltration. The milling was performed with a 600 pA, 30 kV Ga ion beam. It can be seen from Figure 1a that there were many

"crack-like" features distributed throughout the cross section of the pure CNT fiber. These features (Figure 1b) resulted from the separation of CNT bundles within the fiber, which is an indication of poor interactions between the bundles. However, compared to the FIB sections of a pure CNT fiber without solvent densification,[28] the CNT fiber in this study appeared to be much better consolidated and loose CNT ends were hardly observed. This is probably due to the densification effect of ethanol, which was applied at the tip of the triangular CNT ribbon during the fiber spinning.[26] As the ethanol evaporated, the densification effect was realized. After resin infiltration, the CNT fiber shows solid appearance (Figure 1c), even though some crack-like features can still be observed (Figure 1d). This comparison of the cross-sectional morphologies of the CNT fiber before and after resin infiltration indicates that the epoxy resin has effectively penetrated into the void space between CNT bundles in the fiber, which was vital for enhancing the tensile and compressive properties of CNT–epoxy composite fibers reported in the following.

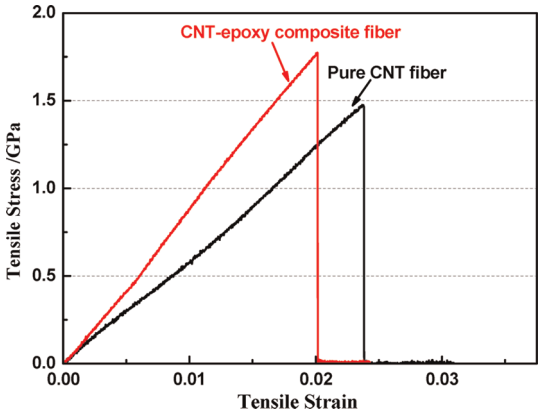

Figure 2. Representative tensile stress–strain curves for a pure CNT fiber and a CNT–epoxy composite fiber.

Single-Fiber Tensile Tests. The mechanical properties of pure CNT fibers and CNT–epoxy composite fibers were characterized by INSTRON 5848 Micro Tester with a gauge length of 7 ± 1 mm, and their tensile properties are summarized in Figure 2. After resin infiltration, the tensile strength of CNT fibers increased from 1.40 ± 0.04 to 1.77 ± 0.14 GPa and the modulus increased from 66.0 ± 1.35 to 93.4 ± 2.87 GPa, while the strain to failure decreased from 2.54 ± 0.17 to 1.99 ± 0.18%. This enhancement in mechanical performance of the CNT–epoxy composite fiber is attributed to the effective infiltration of the epoxy resin into the void space

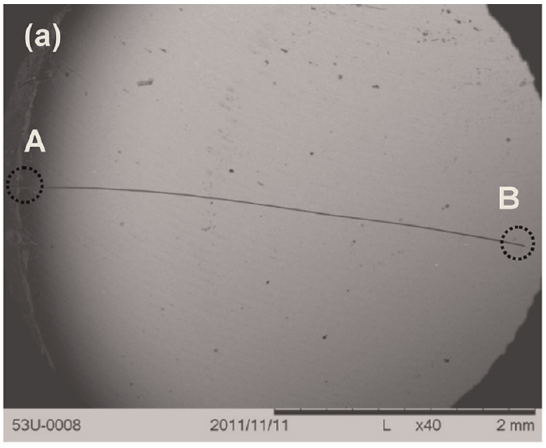

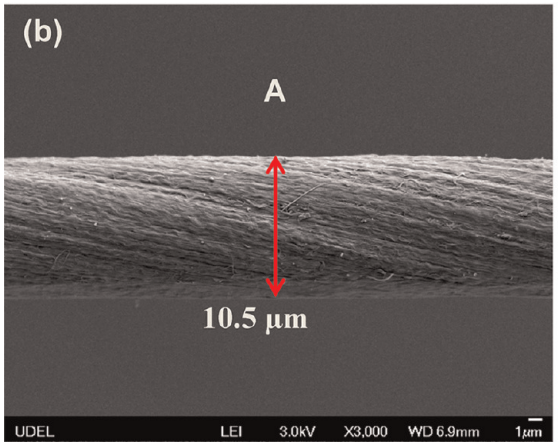

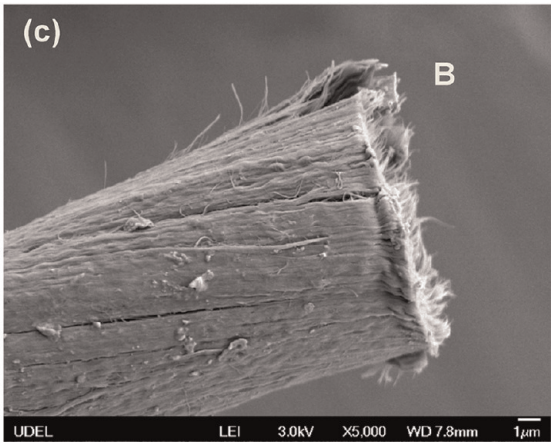

Figure 3. Surface morphology of pure CNT fiber after recoil test at low initial tensile stress of 167.9 MPa. (a) Overall view of the upper segment of the specimen. (b) Location A near the clamp. (c) Location B at fiber cut end.

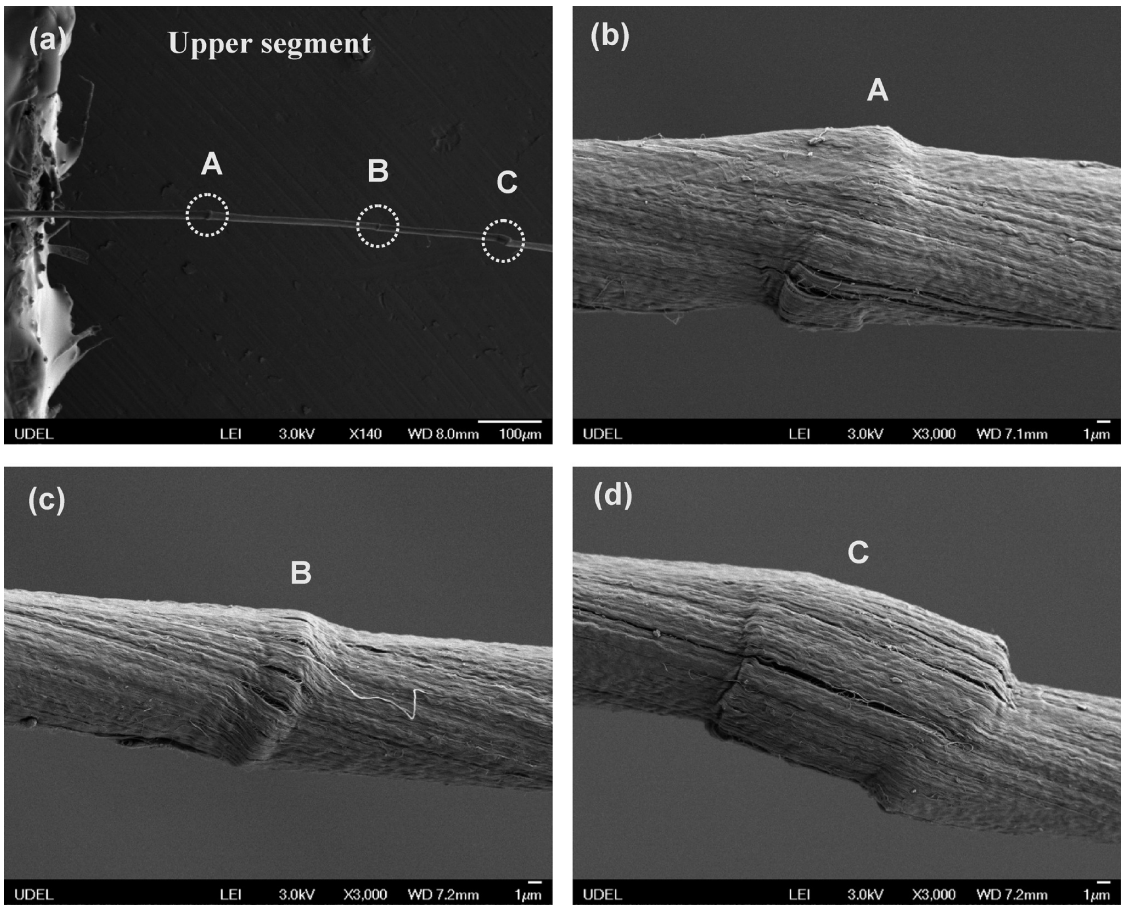

Figure 4. Surface morphology of pure CNT fiber after recoil test at intermediate initial tensile stress of 680.5 MPa. (a) Overall view of the upper specimen segment, (b,c,d) compressive damages at locations away from the clamped end.

within the pure CNT fiber, which was confirmed by the FIB/SEM images. The resin infiltration enabled formations of couplings between CNTs and epoxy resin after curing, resulting in an increase in the load transfer to the CNTs.[29]

Recoil Compressive Tests. Specimens for recoil compressive tests were the same as those used in quasi-static tensile measurements. After a static tensile load was applied to the fiber, the fiber recoil was initiated by cutting the fiber at the midpoint of the gauge length using ultrafine clipper scissors (Fine Science Tools (USA), Inc.) prior to fiber tensile failure. Unlike in the recoil compressive tests of traditional fibers such as Kevlar[20] and carbon fiber,[23] it is not feasible to load and hold the CNT fiber to a predetermined load level. This is due to the fact that slippage among CNT bundles within the fiber takes place when the fiber is held at a constant load, resulting in a gradual load drop (Figure S1 in Supporting Information). Therefore, great care has been exercised to cut the fiber at a desired load level. After cutting a fiber specimen, both fiber pieces (upper fiber segment and lower fiber segment) were carefully removed from the clamps. A determination was then made whether or not compressive damage occurred by examining the fiber ends near where they were clamped using a tabletop SEM (Hitachi TM 100 scanning electron microscope), resulting in two observations per test specimen.

During the recoil test, large increases (spikes) in the applied load will occur if fiber cutting is not done properly. These spikes are usually attributed to the fact that if the two blades of the scissors do not cut the fiber in a symmetrical and balanced manner, that is, both blades are not brought into contact with the fiber at the same instant, the fiber is displaced laterally, causing large increase in the fiber axial load. If the spike is significant, the test is considered to be invalid because the exact stress state in the fiber becomes unknown.[30] Therefore, extreme care has to be exercised for cutting the fiber symmetrically. A scissors mount was installed for stabilizing the scissors during the cutting action. In this study, a "valid test" is defined as a test in which the load spikes less than 10% during cutting. Examples of valid and invalid recoil test specimens are illustrated in Figure S2. Out of the 90 pure CNT fiber specimens tested, 28 specimens yielded valid data, resulting in a success rate of around 30% in properly cutting the fibers under load.

According to the method developed by Allen,[20] under the assumption of no energy dissipation, the

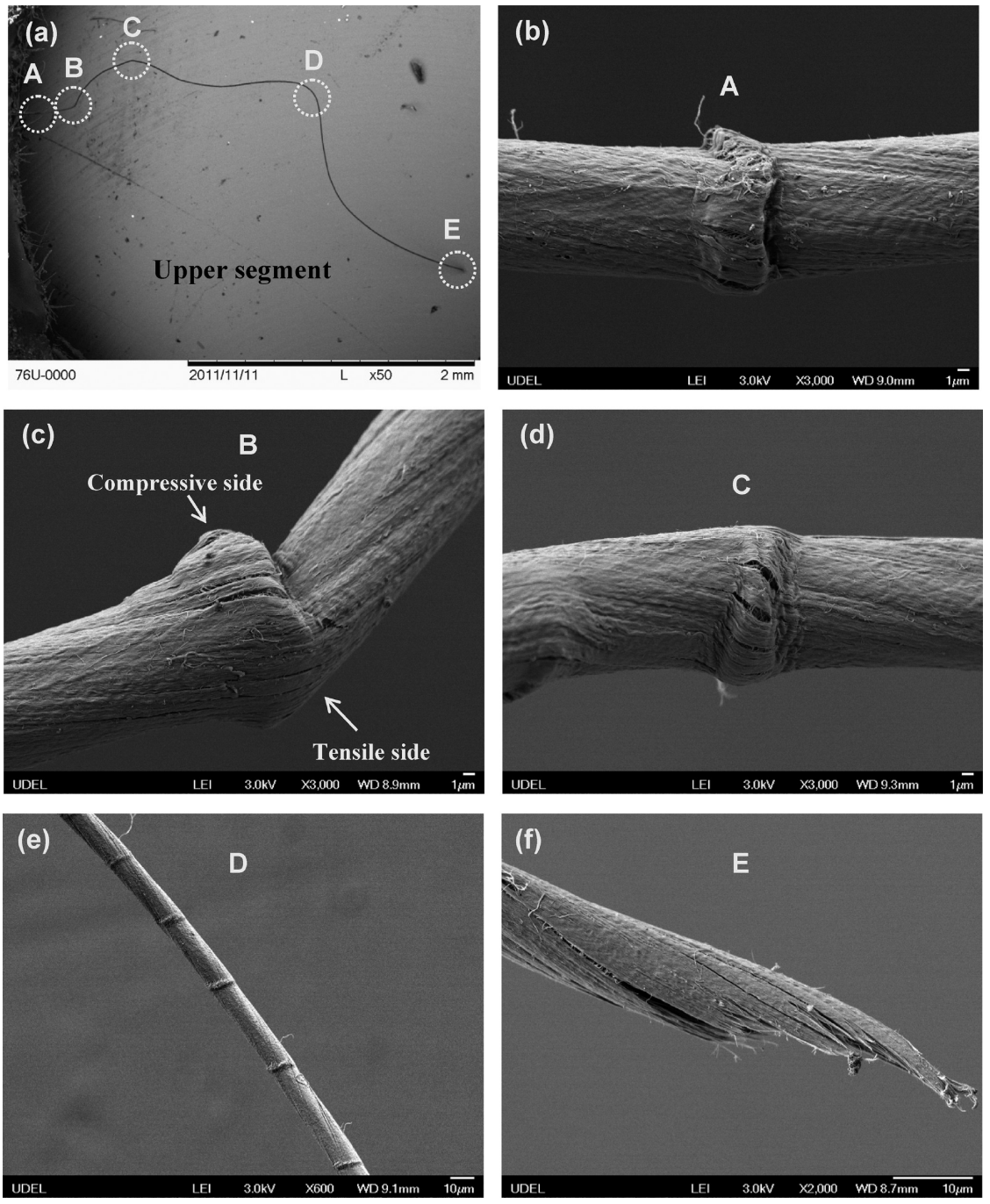

Figure 5. Surface morphology of pure CNT fiber after recoil test at tensile failure stress of 1.48 GPa. (a) Overall view of the upper specimen segment, (b–e) compressive damages at locations (A–D) away from the clamp end and (f) fiber fracture end.

magnitude of the compressive stress wave generated during a specimen recoil is equal in magnitude to but of opposite sign to the initial tensile stress. After performing a number of tensile recoil tests, the threshold stress value just sufficient to induce recoil compressive damage was identified from a ranking of the initial tensile stresses. Data of the 28 valid tests are arranged in an ascending order of the initial tensile stress, as shown in Table S1. Each entry in Table S1 is for a single specimen from which two observations of the upper and lower segments were made. A range of applied stresses is identified over which the observed deformation mode changes from 100% no compressive damage to 100% compressive damage (as marked by the dashed frame). Then, the recoil compressive strength is calculated as the average of the highest and lowest stress values in this range. Therefore, the recoil compressive strength of the CNT fiber in this study was around 416.2 MPa, which was the average of the stress at which the first kink band occurred, 354.1 MPa, and the stress at which the last observation of no compressive damage was recorded,

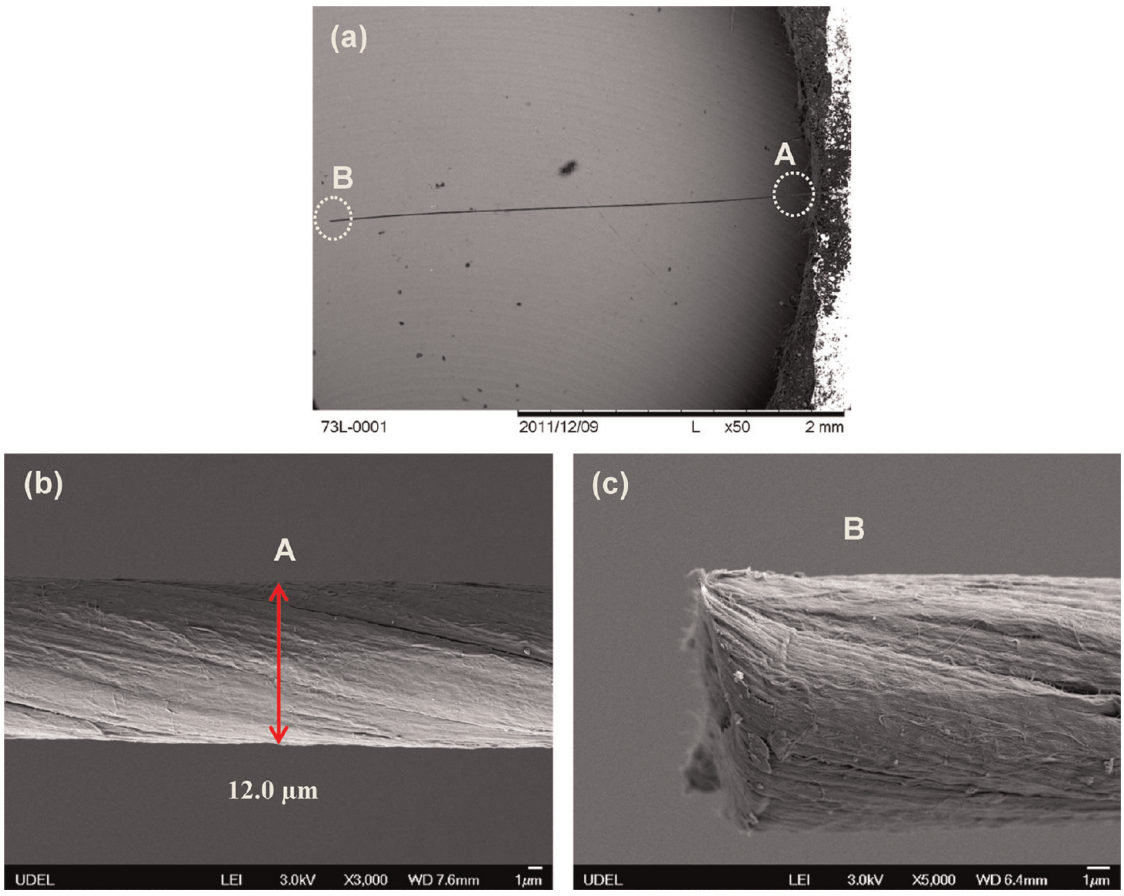

Figure 6. Surface morphology of CNT–epoxy composite fiber after recoil test at low initial tensile stress of 476.4 MPa. (a) Overall view of the lower segment of the specimen. (b) Location A near the clamp. (c) Location B at composite fiber cut end.

478.3 MPa. Individual data point which appears to be an outlier (the compressive failure observed at 275.1 MPa) was excluded from consideration to minimize bias. The value of recoil compressive strength of CNT fiber so determined is comparable to that of Thornel P130 carbon fiber (410 MPa)[23] but higher than those of Kevlar-49 (365 MPa)[20] and aerogel-spun CNT fibers (172–177 MPa);[25] all of them were obtained using the tensile recoil measurement. It is of interest to note that the disparity in the recoil compressive strengths between the two CNT fibers in this study and in ref 25 is attributed to their structural difference resulting from fiber-spun methods. For CNT–epoxy composite fibers, 80 specimens were tested and 25 of them yielded valid data (Table S2). Using the same test method as for pure fibers, the calculated recoil compressive strength is around 573 MPa, which is 37.7% higher than that of the pure CNT fiber. The enhanced compressive strength coupled with the improvement in the tensile strength is due to the effectiveness of resin infiltration (Figure 1).

SEM Examination of Recoil Failure Surfaces. In order to gain insight into the recoil compressive failure of CNT fibers before and after resin infiltration, SEM was used to examine the recoil failure surfaces of the pure CNT fiber and the CNT–epoxy composite fiber. Figures 3–5 illustrate the surface morphologies of pure CNT fibers after tensile recoil from various initial tensile loadings. For low initial tensile stress of 167.9 MPa, there is no obvious recoil damage whether near the clamp or in the rest of the cut fiber, as shown in Figure 3a,b. In addition, Figure 3c shows an SEM image of the cut site (location B), indicating a clean cut by the scissors. At higher initial stress of 680.5 MPa, compressive damage near the clamped end can be easily identified and three kinked locations along the upper specimen segment are shown in Figure 4a–d. When the fiber was broken under axial tensile loading without cutting, the recoil stress reached the tensile failure stress of 1.48 GPa. In this case, massive kinking and severe buckling of the fiber were observed, as shown in Figure 5a–e, and the tensile fracture end of the fiber is shown in Figure 5f. Particularly, it can be seen from Figure 5c that there is no obvious tensile damage on the tensile side of the buckled fiber, while on the compressive side, fully developed kink band and cracking can be found. One possible explanation for this phenomenon is that interactions among the CNTs in the fiber are through the weak van der Waals force. Upon kink deformation of the fiber, CNT bundles on the tensile side of the kink could easily slip with respect to one another, which effectively dissipates the strain

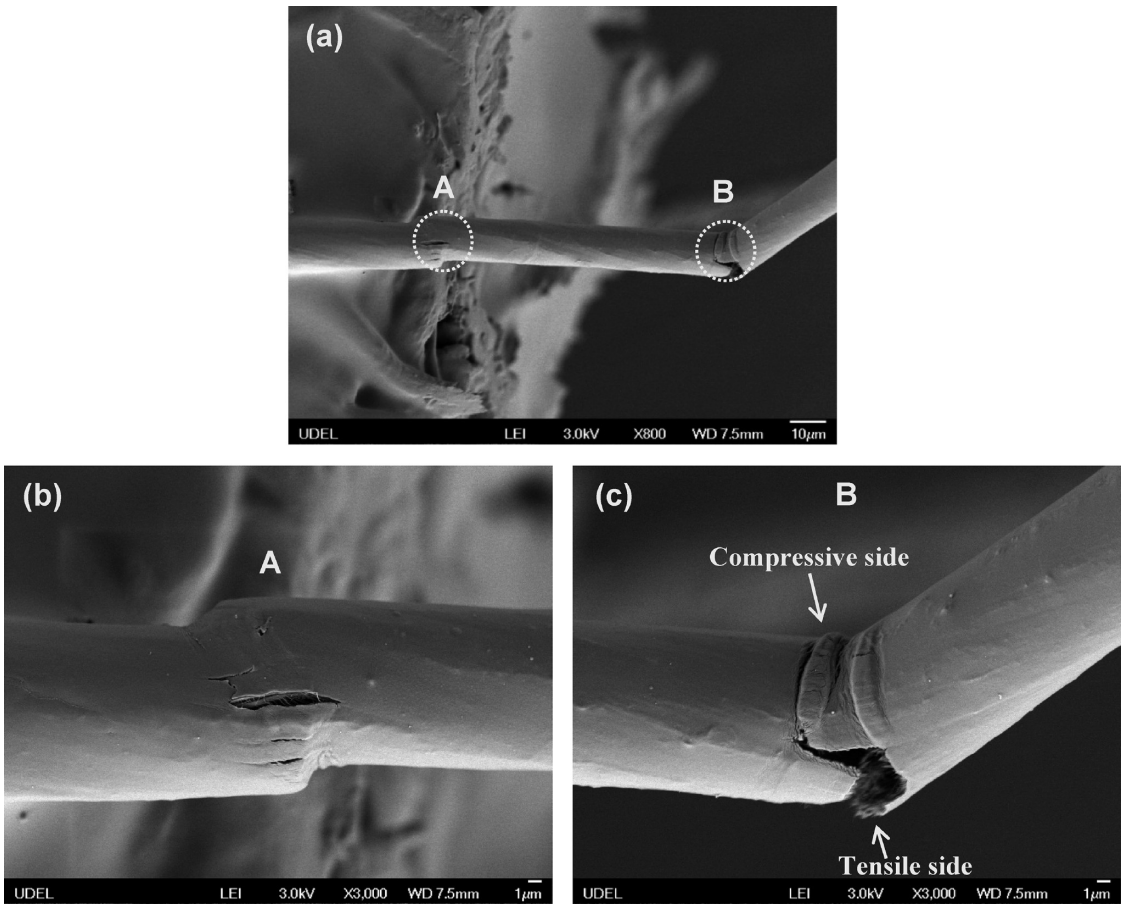

Figure 7. Surface morphology of CNT−epoxy composite fiber after recoil test at intermediate initial tensile stress of 762.6 MPa. (a) Overall view of the upper specimen segment, (b,c) at locations away from the clamp end.

energy and consequently inhibits brittle fracture at the tensile side of the buckled fiber. Meanwhile, on the compressive side, the buckled CNT bundles debonded from one another due to their weak intertube bonding force, giving rise to the interbundle cracks.

On the basis of these microscopic observations, it can be concluded that the recoil failure of the pure CNT fiber occurred in the kinking mode. It should be noted that compressive damage of the specimens in the tensile recoil tests usually takes place near the clamped end, and no obvious damage is observed at distances far away from the clamped end. As can be seen from Figure 5e, although massive kinking was observed at location D resulting in the "bamboo-like" appearance, the deformation associated with the kinking was less severe than that of the kinking observed near the clamped end in Figure 5a,b. In addition, there was no obvious compressive damage observed from location D to location E at the fiber fracture end. As it was concluded by Allen,[20] the compressive stress wave propagates from the clamped end toward the free end. As compressive damages develop in the fiber, the intensity of the propagating compressive stress wave diminishes due to the damage-induced energy dissipation. So at distances far away from the clamped end, the compressive stress level could become inadequate in causing any further damage.

Figures 6−8 illustrate the surface morphologies of the CNT−epoxy composite fibers after tensile recoil from various initial tensile loadings. For the low initial tensile stress of 476.4 MPa, no obvious recoil damage was observed in the upper and lower segments of the specimen (Figure 6a). Due to resin infiltration, the diameter of the CNT fiber is slightly increased from 10.5 μm (Figure 3b) to 12.0 μm (Figure 6b). In addition, a clean fiber cut can be seen in Figure 6c in the case of the CNT−epoxy composite fiber. At the higher initial stress of 762.6 MPa, compressive damage at the clamped ends (both upper segment and lower segment) can be easily identified, and the compressive damage in the upper segment is shown in Figure 7a−c. When the composite fiber was fractured under tensile loading without cutting, that is, the recoil stress reached the tensile failure stress of 1.85 GPa, the upper specimen segment completely fragmented and only a small portion of the lower segment with a length ~400 μm remained (Figure 8a−e). As can be seen in Figure 8b−d, the fiber was severely buckled with formation of cracks on its tensile side.

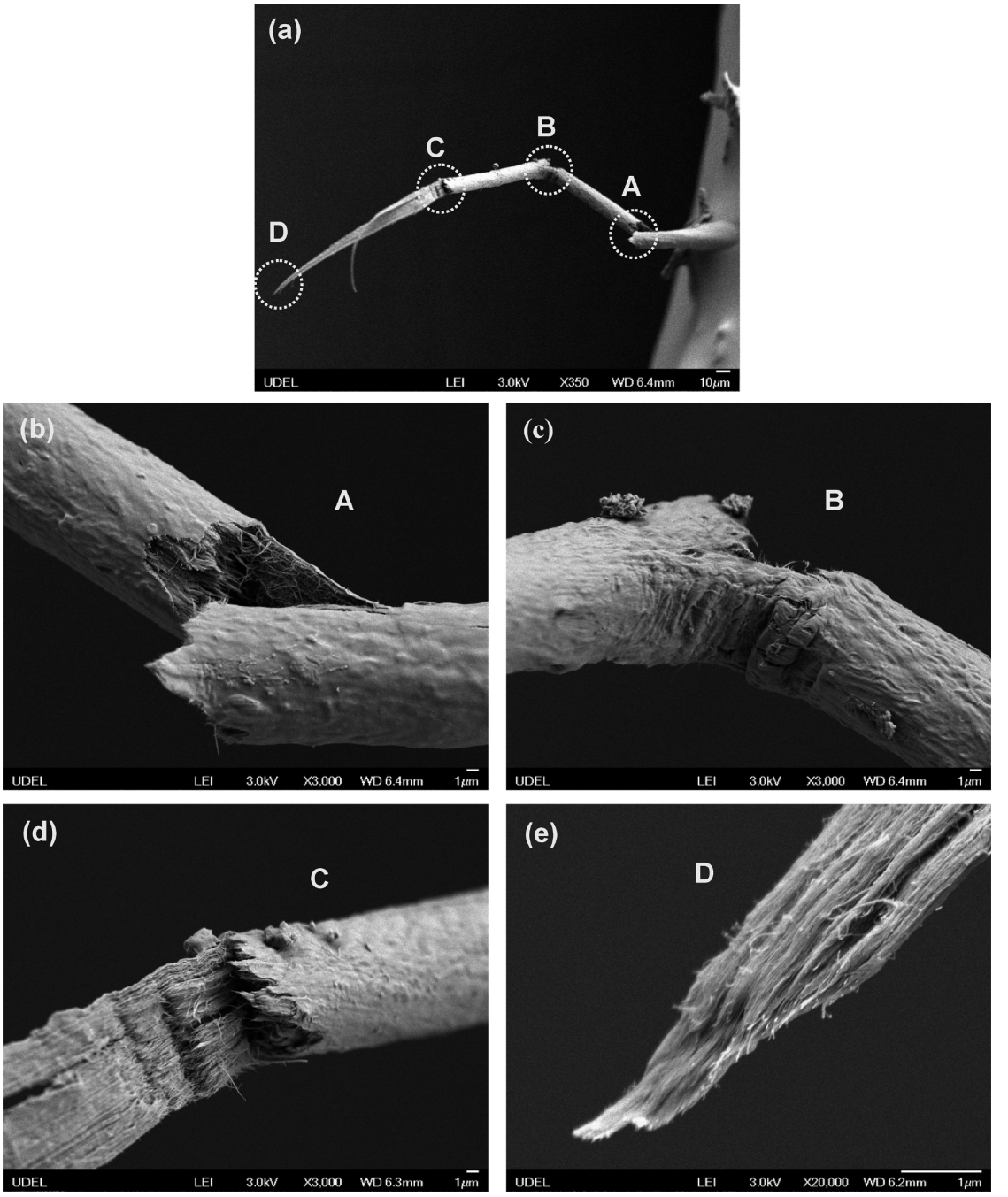

Figure 8. Surface morphology of CNT–epoxy composite fiber after recoil test at tensile failure stress of 1.85 GPa. (a) Overall view of the upper specimen segment, (b–e) locations away from the clamp end.

The buckled CNT–epoxy composite fiber shows a combined tensile and compressive failure surface, which was much like the compressive failure of low modulus pitch-based carbon fibers.[31] Unlike the compressive damage observed in the pure CNT fiber, tensile cracks are observed on the tensile side of the buckled composite fiber, as shown in Figures 7b and 8b,c. This is probably due to the fact that CNT fibers are assemblies of a large amount of individual CNTs, and there exist significant gaps and void space between bundles of CNTs within the fiber, which enables the epoxy resin to infiltrate into the inter-bundle area. After resin infiltration and curing, CNTs are bonded by the epoxy resin. This inhibits the slippage among CNTs and makes the CNT fiber much more brittle, resulting in the formation of tensile cracks once the fiber is buckled. In addition, the enhanced intertube adhesion can well resist the intertube debonding on the compressive side of the buckled composite fiber, impeding the formation of cracks observed on the compressive side of the buckled pure fiber.

CONCLUSIONS

To conclude, the compressive behaviors of both pure CNT fibers and CNT–epoxy composite fibers have been investigated by tensile recoil tests. After epoxy resin infiltration, the mechanical performance of CNT fibers was much improved, with an increase of 26% in the tensile strength and an increase of 38% in the recoil compressive strength. This enhancement is attributed to the effective impregnation of epoxy resin among CNTs, resulting in enhanced interfacial bonding and load transfer to the CNTs. Furthermore, microscopic analysis of the fiber surface morphologies revealed that kinking was the principal compressive failure mode of the pure CNT fiber, while the CNT–epoxy composite fibers exhibited the bending failure mode with a combined tensile and compressive failure surfaces due to the brittleness caused by the epoxy impregnation.

It should be noted that the compressive strength obtained in this study might be overestimated due to the following two considerations. First, there might be some damages underneath the support glue that cannot be detected under SEM.[23] Second, during the recovery of a stretched fiber, the stress at the clamped end cannot be reflected completely and part of the strain energy is dissipated, which results in a smaller compressive stress value compared to the initial tensile stress. In addition, the measured compressive strength of pure CNT fibers in this study is only one-third of their tensile strength. On the basis of the failure mechanism of the CNT fiber, future effort in improving the compressive strength of CNT fibers should focus on enhancing interactions among CNTs in the fiber and improving resin infiltration through surface treatments of the fiber.

This first study of the compressive behavior of CNT fibers using tensile recoil tests expands our knowledge base of the mechanical properties of CNT fibers. Furthermore, the better understanding of the effect of resin infiltration on the single CNT fiber compressive properties, including the compressive strength and the deformation mode, is essential for the application of CNT fibers in multifunctional composites.

MATERIALS AND METHODS

Preparation of CNT–Epoxy Composite Fibers. CNT fibers were first placed in the epoxy bath containing Epon 862 epoxy and Epikure W curing agent at a stoichiometric weight ratio of 100/26.4 and evacuated in a vacuum oven for 1 h at 60 °C. The purpose was to facilitate the removal of microscopic air bubbles trapped among CNT bundles and allow the resin to penetrate fully into the twisted fiber. The composite fiber so fabricated was removed from the bath and placed on a paper towel for soaking up any excess resin. The two ends of the specimen were then mounted on carbon tapes under small tension to ensure its straightness for testing and to force out extra resin for maximizing the fiber volume fraction, followed by a cure cycle of 6 h at 130 °C. Due to the lack of sufficient quantity of CNT fiber in the current study, the fiber volume fraction in the composite fiber could not be measured using traditional methods, such as thermogravimetric analysis (TGA) and quartz crystal microbalance (QCM).

Conflict of Interest: The authors declare no competing financial interest.

Acknowledgment. This work was partially supported by the U.S. Air Force Office of Scientific Research (Dr. Byung-Lip Lee, Program Director) and the Korea Foundation for International Cooperation of Science & Technology (KICOS) through a grant provided by the Korean Ministry of Education, Science and Technology (MEST). M.Z.'s study abroad at the University of Delaware is supported by the State Scholarship Fund of the China Scholarship Council. The authors thank Dr. Amanda Wu for general discussions on fiber testing methods. Dr. Fei Deng's help in CNT fiber cross section characterization using FIB-SEM is also appreciated.

Supporting Information Available: Tables S1 and S2, Figures S1 and S2. This material is available free of charge *via* the Internet at http://pubs.acs.org.

REFERENCES AND NOTES

1. Chou, T. W.; Gao, L. M.; Thostenson, E. T.; Zhang, Z. G.; Byun, J. H. An Assessment of the Science and Technology of Carbon Nanotube-Based Fibers and Composites. *Compos. Sci. Technol.* **2010**, *70*, 1–19.
2. Lu, W.; Zu, M.; Byun, J.-H.; Kim, B.-S.; Chou, T.-W. State of the Art of Carbon Nanotube Fibers: Opportunities and Challenges. *Adv. Mater.* **2012**, *24*, 1805–1833.
3. Liu, L. Q.; Ma, W. J.; Zhang, Z. Macroscopic Carbon Nanotube Assemblies: Preparation, Properties, and Potential Applications. *Small* **2011**, *7*, 1504–1520.
4. Vigolo, B.; Penicaud, A.; Coulon, C.; Sauder, C.; Pailler, R.; Journet, C.; Bernier, P.; Poulin, P. Macroscopic Fibers and Ribbons of Oriented Carbon Nanotubes. *Science* **2000**, *290*, 1331–1334.
5. Ericson, L. M.; Fan, H.; Peng, H. Q.; Davis, V. A.; Zhou, W.; Sulpizio, J.; Wang, Y. H.; Booker, R.; Vavro, J.; Guthy, C.; *et al.* Macroscopic, Neat, Single-Walled Carbon Nanotube Fibers. *Science* **2004**, *305*, 1447–1450.
6. Dalton, A. B.; Collins, S.; Munoz, E.; Razal, J. M.; Ebron, V. H.; Ferraris, J. P.; Coleman, J. N.; Kim, B. G.; Baughman, R. H. Super-Tough Carbon-Nanotube Fibres. *Nature* **2003**, *423*, 703–703.
7. Li, Y. L.; Kinloch, I. A.; Windle, A. H. Direct Spinning of Carbon Nanotube Fibers from Chemical Vapor Deposition Synthesis. *Science* **2004**, *304*, 276–278.
8. Zhong, X. H.; Li, Y. L.; Liu, Y. K.; Qiao, X. H.; Feng, Y.; Liang, J.; Jin, J.; Zhu, L.; Hou, F.; Li, J. Y. Continuous Multilayered Carbon Nanotube Yarns. *Adv. Mater.* **2010**, *22*, 692–696.
9. Koziol, K.; Vilatela, J.; Moisala, A.; Motta, M.; Cunniff, P.; Sennett, M.; Windle, A. High-Performance Carbon Nanotube Fiber. *Science* **2007**, *318*, 1892–1895.
10. Zhang, M.; Atkinson, K. R.; Baughman, R. H. Multifunctional Carbon Nanotube Yarns by Downsizing an Ancient Technology. *Science* **2004**, *306*, 1358–1361.
11. Liu, K.; Sun, Y. H.; Lin, X. Y.; Zhou, R. F.; Wang, J. P.; Fan, S. S.; Jiang, K. L. Scratch-Resistant, Highly Conductive, and High-Strength Carbon Nanotube-Based Composite Yarns. *ACS Nano* **2010**, *4*, 5827–5834.
12. Jiang, K. L.; Li, Q. Q.; Fan, S. S. Nanotechnology: Spinning Continuous Carbon Nanotube Yarns-Carbon Nanotubes Weave Their Way into a Range of Imaginative Macroscopic Applications. *Nature* **2002**, *419*, 801.

13. Zhang, X. F.; Li, Q. W.; Holesinger, T. G.; Arendt, P. N.; Huang, J. Y.; Kirven, P. D.; Clapp, T. G.; DePaula, R. F.; Liao, X. Z.; Zhao, Y. H.; *et al.* Ultrastrong, Stiff, and Lghtweight Carbon-Nanotube Fibers. *Adv. Mater.* **2007**, *19*, 4198–4201.
14. Boncel, S.; Sundaram, R. M.; Windle, A. H.; Koziol, K. K. K. Enhancement of the Mechanical Properties of Directly Spun CNT Fibers by Chemical Treatment. *ACS Nano* **2011**, *5*, 9339–9344.
15. Deng, F.; Lu, W. B.; Zhao, H. B.; Zhu, Y. T.; Kim, B. S.; Chou, T. W. The Properties of Dry-Spun Carbon Nanotube Fibers and Their Interfacial Shear Strength in an Epoxy Composite. *Carbon* **2011**, *49*, 1752–1757.
16. Zu, M.; Li, Q.; Zhu, Y.; Dey, M.; Wang, G.; Lu, W.; Deitzel, J. M.; Gillespie, J. W., Jr; Byun, J.-H.; Chou, T.-W. The Effective Interfacial Shear Strength of Carbon Nanotube Fibers in an Epoxy Matrix Characterized by a Microdroplet Test. *Carbon* **2012**, *50*, 1271–1279.
17. Kozev, V. V.; Jiang, H.; Mehta, V. R.; Kumar, S. Compressive Behavior of Materials: Part II. High Performance Fibers *J. Mater. Res.* **1995**, *10*, 1044–1061.
18. Sinclair, D. A Bending Method for Measurement of the Tensile Strength and Young's Modulus of Glass Fibers. *J. Appl. Phys.* **1950**, *21*, 380–386.
19. Deteresa, S.; Allen, S.; Farris, R.; Porter, R. Compressive and Torsional Behaviour of Kevlar 49 Fibre. *J. Mater. Sci.* **1984**, *19*, 57–72.
20. Allen, S. R. Tensile Recoil Measurement of Compressive Strength for Polymeric High-Performance Fibers. *J. Mater. Sci.* **1987**, *22*, 853–859.
21. Hawthorne, H. M.; Teghtsoonian, E. Axial Compression Fracture in Carbon Fibres. *J. Mater. Sci.* **1975**, *10*, 41–51.
22. Gao, Y.; Li, J. Z.; Liu, L. Q.; Ma, W. J.; Zhou, W. Y.; Xie, S. S.; Zhang, Z. Axial Compression of Hierarchically Structured Carbon Nanotube Fiber Embedded in Epoxy. *Adv. Funct. Mater.* **2010**, *20*, 3797–3803.
23. Hayes, G.; Edie, D.; Kennedy, J. The Recoil Compressive Strength of Pitch-Based Carbon Fibres. *J. Mater. Sci.* **1993**, *28*, 3247–3257.
24. Dobb, M. G.; Johnson, D. J.; Park, C. R. Compressional Behavior of Carbon-Fibers. *J. Mater. Sci.* **1990**, *25*, 829–834.
25. Wu, A. S.; Chou, T.-W.; Gillespie, J. W.; Lashmore, D.; Rioux, J. Electromechanical Response and Failure Behaviour of Aerogel-Spun Carbon Nanotube Fibres under Tensile Loading. *J. Mater. Chem.* **2012**, *22*, 6792–6798.
26. Jia, J. J.; Zhao, J. N.; Xu, G.; Di, J. T.; Yong, Z. Z.; Tao, Y. Y.; Fang, C. O.; Zhang, Z. G.; Zhang, X. H.; Zheng, L. X.; Li, Q. W. A Comparison of the Mechanical Properties of Fibers Spun From Different Carbon Nanotubes. *Carbon* **2011**, *49*, 1333–1339.
27. Bogdanovich, A. E.; Bradford, P. D. Carbon Nanotube Yarn and 3-D Braid Composites. Part I: Tensile Testing and Mechanical Properties Analysis. *Composites, Part A* **2010**, *41*, 230–237.
28. Tran, C. D.; Lucas, S.; Phillips, D. G.; Randeniya, L. K.; Baughman, R. H.; Tran-Cong, T. Manufacturing Polymer/Carbon Nanotube Composite Using a Novel Direct Process. *Nanotechnology* **2011**, *22*, 145302.
29. Ma, W. J.; Liu, L. Q.; Zhang, Z.; Yang, R.; Liu, G.; Zhang, T. H.; An, X. F.; Yi, X. S.; Ren, Y.; Niu, Z. Q.; *et al.* High-Strength Composite Fibers: Realizing True Potential of Carbon Nanotubes in Polymer Matrix through Continuous Reticulate Architecture and Molecular Level Couplings. *Nano Lett.* **2009**, *9*, 2855–2861.
30. McGarry, F. J.; Moalli, J. E. Mechanical Behaviour of Rigid Rod Polymer Fibres: 1. Measurement of Axial Compressive and Transverse Tensile Properties. *Polymer* **1991**, *32*, 1811–1815.
31. Hayes, G. J.; Edie, D. D.; Kennedy, J. M. The Recoil Compressive Strength of Pitch-Based Carbon-Fibers. *J. Mater. Sci.* **1993**, *28*, 3247–3257.